Mapping Wind Farm Loads and Power Production – A Case Study on Horns Rev 1

Christos Galinos[1], Nikolay Dimitrov[1,3], Torben J Larsen[1,2], Anand Natarajan[1] and Kurt S Hansen[1]

[1] Technical University of Denmark, Department of Wind Energy, Frederiksborgvej 399, 4000 Roskilde, Denmark
[2] E-mail: tjul@dtu.dk
[3] E-mail: nkdi@dtu.dk

Abstract. This paper describes the development of a wind turbine (WT) component lifetime fatigue load variation map within an offshore wind farm. A case study on the offshore wind farm Horns Rev I is conducted with this purpose, by quantifying wake effects using the Dynamic Wake Meandering (DWM) method, which has previously been validated based on CFD, Lidar and full scale load measurements. Fully coupled aeroelastic load simulations using turbulent wind conditions are conducted for all wind directions and mean wind speeds between cut-in and cut-out using site specific turbulence level measurements. Based on the mean wind speed and direction distribution, the representative 20-year lifetime fatigue loads are calculated. It is found that the heaviest loaded WT is not the same when looking at blade root, tower top or tower base components. The blade loads are mainly dominated by the wake situations above rated wind speed and the highest loaded blades are in the easternmost row as the dominating wind direction is from West. Regarding the tower components, the highest loaded WTs are also located towards the eastern central location. The turbines with highest power production are, not surprisingly, the ones facing a free sector towards west and south. The power production results of few turbines are compared with SCADA data. The results of this paper are expected to have significance for operation and maintenance planning, where the schedules for inspection and service activities can be adjusted to the requirements arising from the varying fatigue levels. Furthermore, the results can be used in the context of remaining fatigue lifetime assessment and planning of decommissioning.

1. Introduction and work objectives

In large wind farms the loading and power production of individual turbines can vary significantly depending on the turbine location in the park due to the effect of wakes or variations in the free-wind conditions. Nevertheless, the turbines in a wind farm typically have identical rotor-nacelle assemblies designed to withstand wind conditions corresponding to a reference design class, and consideration of the site-specific conditions is only given to the extent that ensures the loads on the worst-affected turbine in the farm do not exceed the design limit. An exception to this approach are the support structures which are specifically tailored to different turbine positions. As a result, the fatigue loads accumulated by turbine structures can vary significantly. Mapping the variation of fatigue load exposure on farm level is relevant for a number of engineering purposes such as prediction of reliability, enabling O&M service to start with the highest loaded turbines, or estimating the remaining fatigue lifetime of currently operational wind farms.

The present study utilizes the dynamic wake meandering model [1, 2] to calculate wind conditions in the wake, integrated within the HAWC2 aeroelastic simulation tool [3] to determine the fatigue damage equivalent loads and power production of the Horns Rev 1 (HR1) wind farm. Lifetime fatigue loads are predicted for each wind turbine (WT), by considering a representative set of design situations, which take into account the influence of site-specific environmental conditions. The following factors are considered:

- Ten-minute average free wind speed
- Free wind direction
- Ambient turbulence
- Farm layout and wake effects
- Wave height, peak period, and alignment with the wind.

This setup allows characterizing the fatigue load variation within the wind farm for multiple WT components. Assuming identical turbines are used in the entire farm, and taking the load levels simulated under IEC class 1A conditions as a design reference, the fraction of fatigue capacity that is used over the 20-year lifetime can be estimated for each turbine at HR1.

2. Estimation of wake effects by aeroelastic simulations

The HR1 wind farm comprises of 80 Vestas V80 wind turbines which are placed in a regular array of 10 columns and 8 rows interspaced with 7D, see Figure 1. The turbines are supported on monopile foundations embedded in the sea floor. The aeroelastic model considers a simplified representation of the foundations, where soil conditions are not taken into account, and the water depth is taken as a constant value of 10m, which is approximately equal to the average water depth at HR1. The wake conditions experienced by a given turbine in a wind farm are a function of the wind direction which determines the set of disturbing turbines, and the ambient turbulence which affects the meandering of the wakes and thus the probability of occurrence of a wake situation.

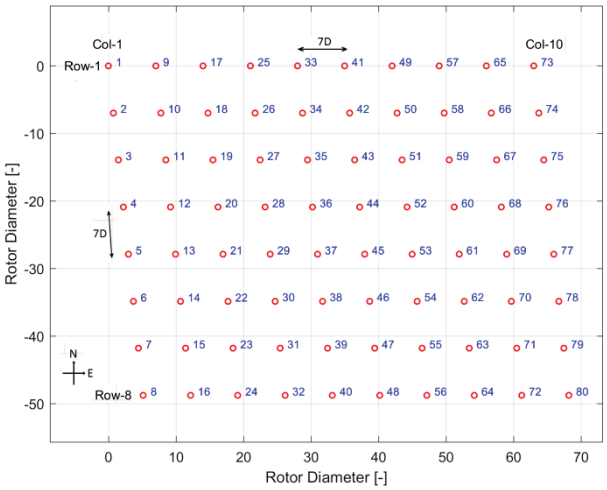

Figure 1. Layout of the Horns Rev 1 wind farm

The DWM model that is used in the DTU HAWC2 code [3] represents the meandering of the wakes generated by wind turbines assuming that they are transported as passive tracers by the large scale atmospheric turbulence structures. A coarse turbulence grid covering the entire wind farm area is used to capture the large scale coherent turbulence structures and acts as a mean for the meandering process of the wake deficits. An additional, small-scale turbulence field represents the wake-induced vorticity. All turbulence fields are based on the Mann turbulence spectral model [4]. The wake deficit is extracted from the Blade Element Momentum (BEM) theory together with axisymmetric thin shear

layer solution of the Navier-Stokes equations [5]. Full scale load validation can be found in [2] and [6]. The DWM model takes into account the contribution of the nearest upstream WT wake up to rated (ambient) wind speeds while it sums linearly the upstream wakes for mean wind speeds above rated [6].

For the calculation of 20 year life time fatigue loads and electrical energy production it is assumed that all the WTs operate throughout the 20 years at full availability and without curtailment. The simulations are carried out from cut-in to cut-out wind speeds with 2m/s steps and 2 degrees discretization in wind direction. In order to allow better characterization of the effect of wake meandering and to reduce statistical uncertainty, each simulation has 30-minute duration instead of the typical 10 minutes. The lifetime damage-equivalent fatigue load is calculated by equation 1 for a given Wöhler exponent m and total expected number of equivalent cycles $n_{eq,L}$.

$$L_{eq} = \left(\frac{\int_U \int_\Theta R_{eq}(U,\Theta)^m n_{eq} n_T p(U,\Theta) dU d\Theta}{n_{eq,L}} \right)^{\frac{1}{m}} \quad (1)$$

A 1-Hz equivalent fatigue load $R_{eq}(U,\Theta)$ is obtained from each simulation, where the duration of each simulation corresponds to $n_{eq} = 1Hz \cdot 1800s = 1800$ equivalent cycles. The joint probability of the combination of mean wind speed and wind direction is denoted as $p(U,\Theta)$, n_T is the number of time series considered for each design condition, and $n_{eq,L}$ is the number of equivalent cycles corresponding to 20 years operation. Although a fatigue design load calculation normally also takes into account the fatigue damage contribution from transient events such as startups, shutdowns and idling at high wind speeds, these conditions are not considered in the present study as it is assumed that for these situations, the total lifetime damage contribution is approximately the same for most of the wind turbines in the wind farm.

A full analysis of all wake-related design situations with one turbulence seed per design condition for all turbines in the HR1 wind farm would require at least 158400 simulations. In order to reduce this requirement, the present analysis exploits the geometric similarities of the wind farm layout (regular spacing of WTs), meaning that there are only certain possible spacing distances between disturbing WTs. This means that the wake loading conditions for the entire park can be characterized as a function of certain variables related to the farm layout and the ambient conditions. The variables used are listed below, with the corresponding ranges given in brackets:

- Mean free wind speed (cut-in to cut-out);
- Ambient turbulence intensity (a 90% quantile representative for load simulations is used, conditional on free wind direction);
- Number of disturbing turbines (from 0 to 9);
- Spacing between the disturbing turbines (7 to 16.3 rotor diameters);
- Angle between the mean wind direction and the upwind turbine location (-20 to +20 degrees).

The five variables listed above are sufficient to fully define the relative position between a turbine in a wind farm and its disturbing neighbours, as well as the wind conditions necessary for estimating IEC standard-compliant, site-specific design loads including wake effects. Defining a functional relation between the input variables and a given design load requires a choice of ranges and values of the inputs. The most appropriate choice of input values will differ from wind farm to wind farm due to the specific farm layouts. For example, for the Horns Rev 1 farm, the distance between any two turbines is exactly 7, 9.3, 10.5, 14.9, 16.3 or 22 rotor diameters, or a multiple of these. Considering only these particular distances will significantly reduce the number of load simulations, but it also means that the resulting load assessment will be valid only for the particular wind farm.

An illustration of the effect of the number of disturbing turbines and the wake angle on the fatigue loads is shown on Figure 2 for mean free wind speed of 15m/s and a spacing of 7 rotor diameters. In

this particular situation, the wake-induced loads increase with the number of disturbing turbines up to about 4 turbines in a row, beyond which the wake influence begins to saturate. For higher mean wind speeds where the turbine thrust coefficient is even lower, more turbine rows are required to reach this saturation effect. Therefore, at high wind speeds up to 9 disturbing turbines are considered in the simulations. The approach of using geometric regularities within the farm reduces the overall number of simulations by 85% compared to a full set of simulations for each turbine in the farm. The functional relation between the above mentioned variables and the damage-equivalent loads is defined in terms of a surrogate model. A similar surrogate model approach is used in [8], Ch.4, for relating the load distribution to the distributions of wind shear and veer. In the present study, the surrogate model is implemented using a Kriging interpolation scheme [7] and the five input variables listed above. The model development proceeds by evaluating an increasing number of sample points within the input variable domain, until sufficient accuracy is achieved. In the present case, the accuracy criterion is based on the mean relative error evaluated using a 5 fold cross-validation procedure. The termination of the surrogate model development occurs when the estimated error is less than 2% of the function value. A comparison of this approach with an actual simulation result for the blade root flapwise load polar at 16m/s for turbine no. 28 is shown on Figure 3.

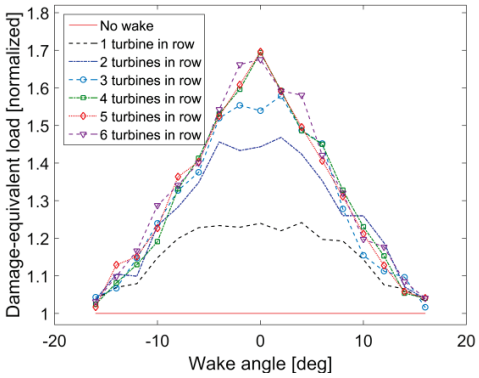

Figure 2. Effect of wakes on blade root flapwise damage-equivalent fatigue loads estimated using the Dynamic Wake Meandering (DWM) model for turbines in a row with 7D spacing, at 15m/s mean wind speed. The loads are normalized with the value from wake-free simulations.

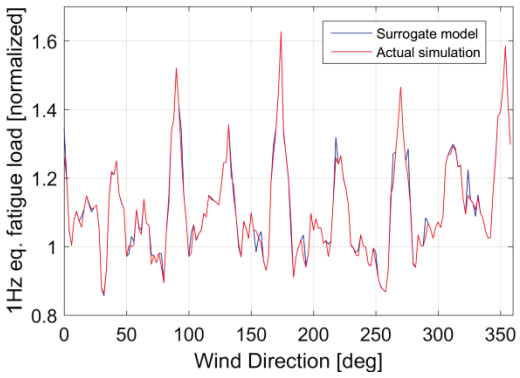

Figure 3. Blade root flapwise 1 Hz equivalent fatigue load as a function of wind direction for WT 28 at 16 m/s wind speed. Comparison of the surrogate model prediction with the actual results. The loads are normalized with the value from wake-free simulations.

3. Distribution of environmental conditions

The meteorological data used to define the statistical distribution of the environmental conditions on the Horns Rev site are taken from a meteorological mast (denoted Mast 2) located to the north-west of the wind farm. Most of the wind parameters can also be estimated or validated from the operational data of the wake-free wind turbines which are equipped with a nacelle anemometer and a wind vane; in addition, the rotor-effective wind speed can be estimated by the power production of wake-free, non-curtailed turbines. Using measurements from Mast 2 over a 3 years period from 2005 to 2007, the statistical distributions of the mean wind speed U, mean wind direction Θ, and turbulence σ_U are estimated based on 10-minute reference periods. In order to simulate wake effects, the mean wind speed and direction distributions are estimated over 2-degree intervals. As the standard deviation of wind speed is a higher-order statistic, the data are not sufficient for such a fine resolution, and the turbulence distribution is estimated over 30-degree sectors. The wind speed is considered Weibull-distributed, the ambient turbulence – Log-normally distributed, while for the wind direction no specific distribution is chosen – a table with the assigned probability of each direction sector is used. Figure 4 shows the polar plots of the wind direction probability, mean wind speed, and characteristic

turbulence at 15m/s. Wave loads are also taken into account by adding irregular Airy waves with significant wave height Hs, varying from 0.8 m at 4 m/s mean wind speed up to 4.7 m at 24 m/s wind speed. Based on [9], the significant wave height is considered as approximately linear function of the free wind speed (Figure 5), while the wave peak crossing period T_p is fully correlated with the significant wave height and as such is also a function of the mean wind speed. Unfortunately, detailed wave climate data for the HR1 wind farm is not available; therefore the Hs and T_p values used are adopted from a similar site. In addition, a characteristic wind-wave misalignment angle of 5 degrees is assumed.

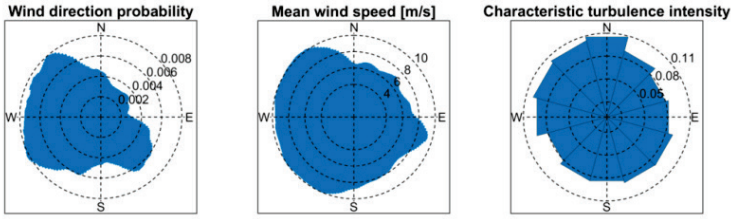

Figure 4. Polar plots of wind condition distributions and statistics at the HR1 wind farm.

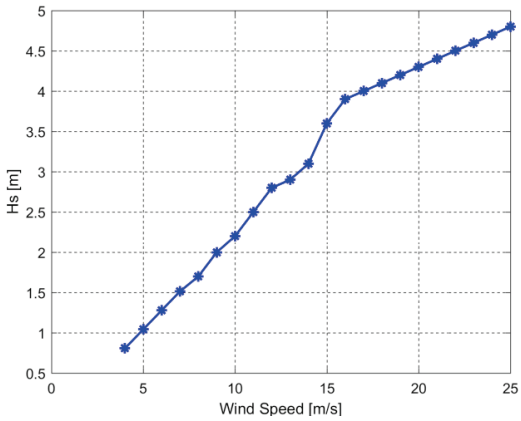

Figure 5. Significant wave height H_s as function of mean wind speed.

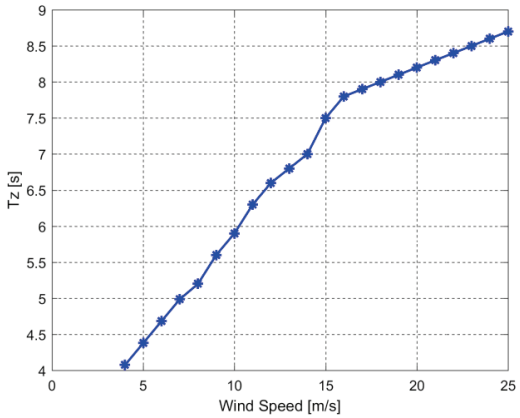

Figure 6. Wave peak crossing period T_z as function of mean wind speed.

4. Results

The 1-Hz damage-equivalent blade root flapwise bending moments (BMs) at 8 m/s and 16 m/s wind speed of the upper left part of the wind farm are plotted on Figure 7 left and right respectively. The results are normalized with the corresponding free sector fatigue load levels which are illustrated by the blue circles, while the actual load level per WT with the red curves. It can be seen that the wake generated loads increase down the rows of wake affected turbines, which is especially pronounced during operation at above rated wind speed (Figure 7 right). The same increase in loads is not seen below rated, because at lower wind speeds the DWM model only considers the wake from the nearest disturbing turbine. This behavior of the DWM model accounts for increased turbulent mixing at lower wind speeds and high thrust coefficients, an approach which has been found to match observations well [6]. Thus, the WTs which are located within columns 3 to 8 and rows 3 to 6, are predicted to have almost the same load level per wind direction at below rated speeds. As shown by the blade root flapwise moment variation on Figure 7, the fatigue loads vary up to 85% over the wind farm under full wake WT operation below rated and more than 100% for wind speeds above rated.

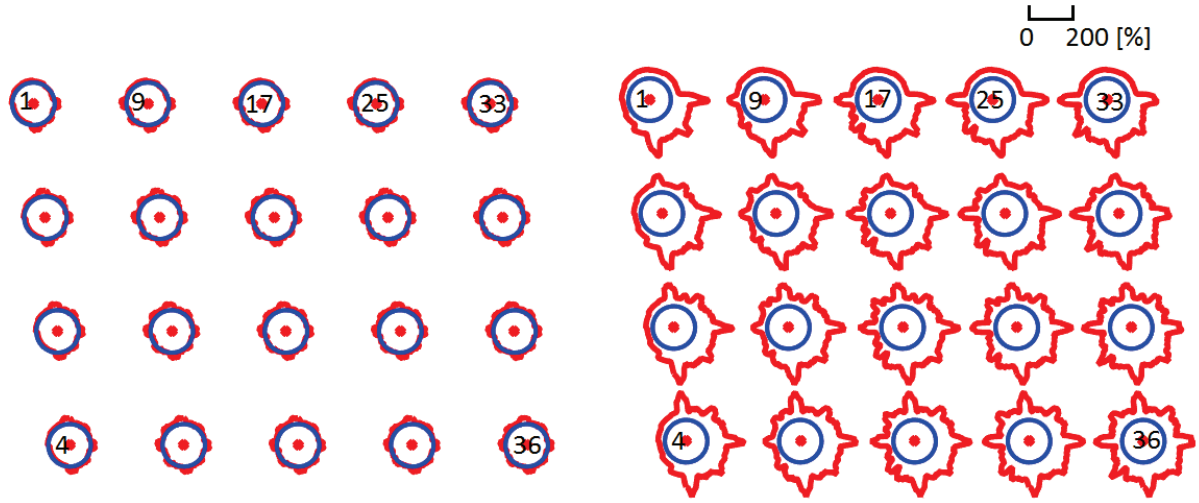

Figure 7. Blade root flapwise 1Hz DEL at 8 m/s on the left plot and at 16 m/s on the right. The values are normalized by the load level of a free sector at 8 m/s (blue circles). The red curves represent the load levels as a function of wind direction. Upper left part of the wind farm.

A few key 20-year lifetime damage-equivalent fatigue load (DEL) results are plotted in Figures 8 to 11. The Wöhler exponents that have been used in the analysis are m=4 for the tower base and monopile structures, m=8 for the tower-top yaw gear system and m=12 for the glass fiber blades. For the blades and the tower base, the load levels are normalized with the load levels corresponding to both the wake free WT load and the IEC 1A wind conditions which is the type-certification level of the Vestas V80 wind turbines installed at HR1. The monopile fatigue load levels are normalized with the loads corresponding to wake-free operation under the site-specific wind conditions. All load levels are compared without applying any safety factors. On Figures 8 to 11, the areas with the most heavily loaded turbines are illustrated with red color. For the blade root flapwise BM (Figure 8) and the tower base fore-aft BM (Figure 9) the most fatigue damage-exposed part of the wind farm is the east-south-east region where due to the prevailing wind directions the WTs operate in wake conditions for a longer period. The 20 years load levels vary up to 18% for the blade root flapwise and up to 30% for the tower base fore-aft when compared with the free wake WT load levels over the wind farm. For the given wind climate, the east-south-east part of the wind farm results in highest fatigue damage for all load components strongly affected by turbulence (e.g. tower base fore-aft and blade root flapwise loads). For the tower top yaw moments (Figure 10) the highest loads are found more centrally in the wind farm with an overall variation in the order of 5%. This however only implies low overall variation of the lifetime accumulated damage; it does not imply that wakes have no effect on the yaw fatigue loads. In some particular cases (e.g. 8m/s wind speed and 7 rotor diameters spacing) the yaw DEL simulated under wake situations is up to 62% higher than the DEL under free wind. For the blade root edgewise bending moment the variation in the lifetime fatigue damage is minimal, which can be expected since the blade edgewise moment is mainly dominated by cyclic gravity-driven loads. The estimated site specific lifetime DELs for the tower and the blades are less than 78% of the corresponding IEC 1A reference loads. The lifetime fore-aft DEL at the mudline for the monopile (Figure 11) has very similar distribution within the wind farm as the tower base fore-aft DEL.

Figure 12 shows the relative lifetime damage contribution per mean wind speed bin, weighted by the wind speed probability distribution, for the highest-loaded WT for three different load sensors: the tower base fore-aft, the tower base side-side and the tower top yaw moments. The mean wind speed probability distribution averaged over all wind directions is also illustrated. The main contribution to the fatigue damage for the tower base fore-aft and tower top yaw moments emerges at moderate to high winds despite that the probability of such wind speeds is relatively low. The same behavior is

observed for the blade root flapwise BM. The increase of fatigue damage at high mean wind speeds is most pronounced for the tower side-side moment. This is mainly due to the side-side moment being affected by wave loads, where the wave height increases proportionally to the mean wind speed, in combination with the absence of aerodynamic damping in the side-side direction.

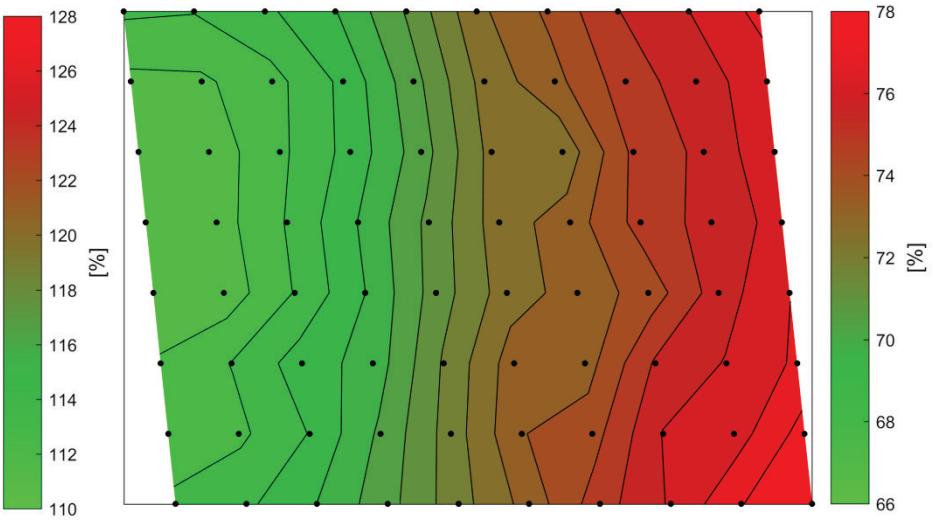

Figure 8. Lifetime DEL for blade root flapwise BM over the wind farm normalized by the wake free WT load level (left bar) and the IEC 1A load level (right bar).

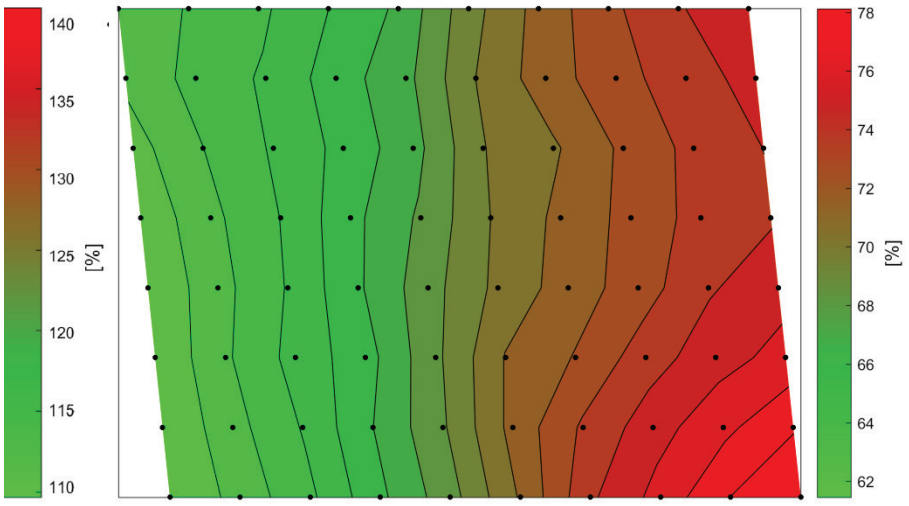

Figure 9. Lifetime DEL for tower base fore-aft BM over the wind farm normalized by the wake free WT load level (left bar) and the IEC 1A load level (right bar).

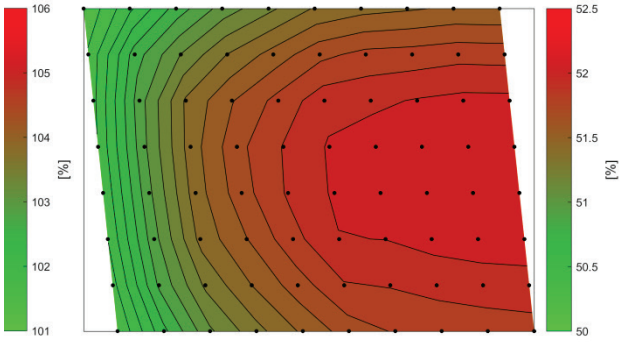

Figure 10. Lifetime DEL for tower top yaw moment normalized by the wake free WT load level (left bar) and the IEC 1A load level (right bar).

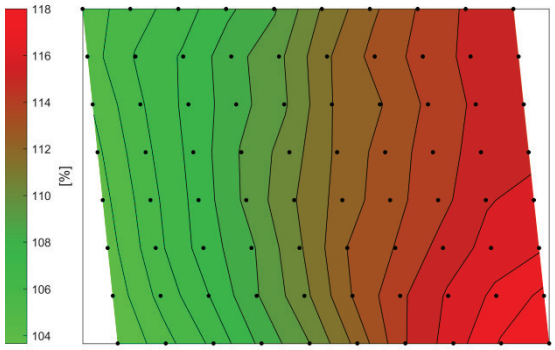

Figure 11. Lifetime DEL for monopile at mud line fore-aft BM normalized by the wake free WT load level.

The Annual Energy Production (AEP) is shown on Figure 13 normalized by the AEP of a stand-alone (without wake effects) WT subjected to the site specific wind climate conditions. The AEP varies up to 9% depending on the WT location within the wind farm. The fact that turbine no. 8 burned down a few years ago is not taken into account in this study. In addition, the AEP results for WT no. 5 and no. 55 are compared with data made available from the WTs SCADA system. They are based on data of six years of operation from 2005 until 2011, excluding year 2008 because recorded data was very low. The recorded AEP per year was converted to full operation AEP (8760 h) and the six year average was compared. The Measured AEP difference between these 2 WTs is 7.6 % while the HAWC2 simulation results predict a difference of 5.1 %, which is considered to be in good agreement.

In the present study it was decided to use the site specific 90% quantile as ambient turbulence intensity level, in order to ensure conservative load estimation, and because for wake-free turbines the 90% quantile of turbulence typically produces approximately the same fatigue loads as the full distribution of turbulence. However, when considering wakes and the effect of wake meandering, additional factors come into play. The turbulent mixing in the wake and the variation of the meandering wake position are both influenced by the ambient turbulence. The fact that the simulated variation in power production is slightly less than the observed variation could imply that lower values for the ambient turbulence intensities, perhaps the mean turbulence level, may need to be used in wake load simulations.

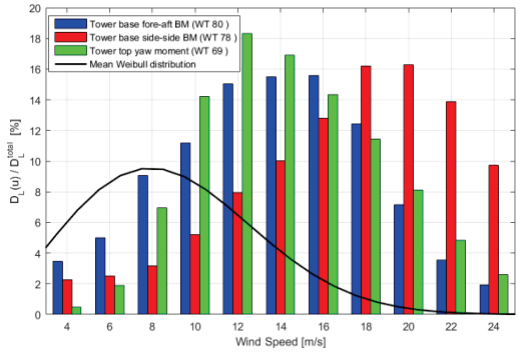

Figure 12. Relative lifetime damage contribution for the highest loaded WT for the tower base fore-aft and side-side BMs and the tower top yaw moment.

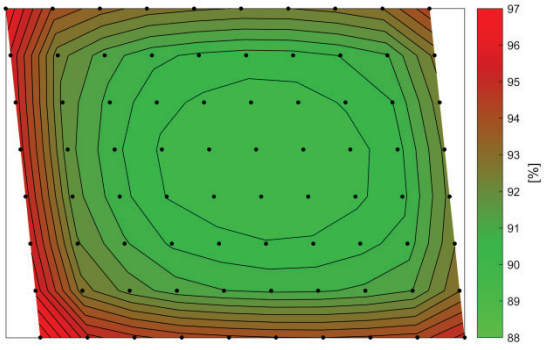

Figure 13. AEP normalized by the wake free WT AEP.

The outcomes of the loads study have important implications concerning planning of Operation and Maintenance (O&M) activities. Knowing the variation of loading conditions within the wind farm makes it possible to adjust inspection and component replacement schedules to prioritize the maintenance of more heavily loaded turbines. The load variation can also be used as a decision basis for choosing specific locations for installing condition monitoring systems. This is especially important in the case of wind farms with closer row spacing as the wake-induced consequences are considerably higher.

5. Conclusions

The present study described the process of obtaining a fatigue load map of the Horns Rev 1 wind farm using a combination of measured wind conditions and aeroelastic simulations. It was observed that the wake effects can cause up to 35% variation in the 20-year damage-equivalent loads throughout the farm. It also showed that the fatigue loading, for the present wind farm, is still lower than the design reference class IEC1A, which indicates that some of the turbine components can survive longer than their intended lifetime. The fatigue damage in the blade root flapwise, the tower base fore-aft and the tower top yaw components is mainly accumulated at moderate to high mean wind speeds. The present work also contributes to facilitating operation and maintenance activities, since the load variation within a wind farm can serve as a decision basis for installation of condition monitoring systems and for scheduling inspection and service activities according to the expected load-induced fatigue damage accumulation.

Acknowledgements

This work has been funded by the Danish Energy Technology Development and Demonstration Programme under contract 64013-0569.

References

[1] Larsen G C, Madsen H A, Thomsen, K. and Larsen T J 2008. Wake meandering - a pragmatic approach. Wind Energy, 11, pp. 377–395.
[2] Larsen T J, Madsen H A, Larsen G C and Hansen K S 2013. Validation of the Dynamic Wake Meander Model for Loads and Power Production in the Egmond aan Zee Wind Farm. Wind Energy, Volume 16, Issue 4, pp. 605–624.
[3] Larsen T J and Hansen A M 2014. How 2 HAWC2, the user's manual, Risø-R-1597(ver.4-5)(EN). Risø National Laboratory, Technical University of Denmark.
[4] Mann J 1994. The spatial structure of neutral atmospheric surface-layer turbulence. Journal of Fluid Mechanics, 273:141-168.
[5] Madsen H A, Larsen G C, Larsen T J, and Troldborg N 2010. Calibration and Validation of the Dynamic Wake Meandering Model for Implementation in an Aeroelastic Code. J. Sol. Energy Eng., 132(4).
[6] Larsen T J, Larsen G C, Madsen H A, and Petersen S M 2015. Wake effects above rated wind speed. An overlooked contributor to high loads in wind farms. EWEA conference, Paris.
[7] Gorissen D, Couckuyt I, Demeester P, Dhaene T, and Crombecq K, 2010. A surrogate modeling and adaptive sampling toolbox for computer based design. The Journal of Machine Learning Research, 11, pp.2051-2055.
[8] Natarajan, A., Dimitrov, N. K., Madsen, P. H., Berg, J., Kelly, M. C., Larsen, G. C., Thesbjerg, L. (2016). Demonstration of a Basis for Tall Wind Turbine Design, EUDP Project Final Report. DTU Wind Energy. (DTU Wind Energy E; No. 0108)
[9] Natarajan, A. 2014. Influence of second-order wave kinematics on the design loads of offshore wind turbine support structures, Renewable Energy 68, pp. 829-841.